

Water (Non-)Interaction with MoO₃

Ashley R. Head,[†] Chiara Gattinoni,[‡] Lena Trotochaud,^{§,○} Yi Yu,^{§,⊥,◆} Osman Karlioglu,^{§,¶} Sven Pletincx,^{§,¶} Bryan Eichhorn,[⊥] and Hendrik Bluhm^{*,§,||,▽}

[†]Center for Functional Nanomaterials, Brookhaven National Laboratory, Upton, New York 11973, United States

[‡]Materials Theory, Department of Materials, ETH Zürich, Wolfgang-Pauli-Str. 27, 8093 Zürich, Switzerland

[§]Chemical Sciences Division and ^{||}Advanced Light Source, Lawrence Berkeley National Laboratory, Berkeley, California 94720, United States

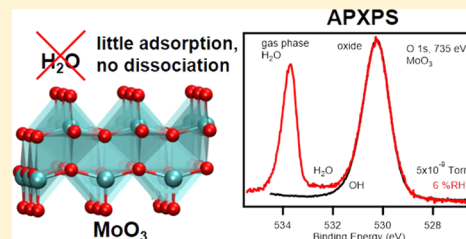
[⊥]Department of Chemistry and Biochemistry, University of Maryland, College Park, Maryland 20742, United States

[#]Department of Materials and Chemistry, Research Group Electrochemical and Surface Engineering (SURF), Vrije Universiteit Brussel, Pleinlaan 2, 1050 Brussels, Belgium

[▽]Department of Inorganic Chemistry, Fritz Haber Institute of the Max Planck Society, Faradayweg 4-6, D-14195 Berlin, Germany

S Supporting Information

ABSTRACT: Molybdenum(VI) oxide (MoO₃) is used in a number of technical processes such as gas filtration and heterogeneous catalysis. In these applications, the adsorption and dissociation of water on the surface can influence the chemistry of MoO₃ and thus the course of heterogeneous reactions. We use ambient pressure X-ray photoelectron spectroscopy to study the interaction of water with a stoichiometric MoO₃ surface and a MoO₃ surface that features oxygen defects and hydroxyl groups. The experimental results are supported by density functional theory calculations. We show that on a stoichiometric MoO₃(010) surface, where Mo sites are unavailable, water adsorption is strongly disfavored. However, the introduction of surface species, which can interact with the lone pairs on the water O atom, e.g., Mo³⁺ atoms or surface OH groups, promotes water adsorption. Dissociation of water is favored at unsaturated Mo sites, i.e., at oxygen vacancies, while water adsorbs molecularly at hydroxyl sites.



1. INTRODUCTION

Water interaction with metal oxide surfaces plays an important role in many processes ranging from electrochemistry and corrosion to environmental chemistry. These interactions include adsorption and dissociation and, in turn, influence other heterogeneous reactions due to the presence of water molecules and hydroxyls.¹ This last point is particularly relevant to air filtration materials used in the removal of toxic organic molecules, such as industrial chemicals and nerve agents. These filtration materials are often composed of porous carbon impregnated with metal oxides.² How these filtration materials, including the metal oxides, interact with ambient water vapor during storage and use is still largely unknown. Of great concern is also how humidity impacts reactions with other atmospheric gases, such as NO_x and SO_x, and thus the effectiveness of air filtration materials under standard application scenarios.

In a recent study of MoO₃, a typically used metal oxide in these filters,² we showed that the presence of oxygen vacancies and surface hydroxyl groups increased the adsorption of the organophosphonate nerve agent simulant dimethyl methyl phosphonate under controlled vacuum conditions.³ In a step toward understanding how relative humidity (RH) affects the surface chemistry, we have studied MoO₃ from ultrahigh vacuum (UHV) to 6% RH using ambient pressure X-ray

photoelectron spectroscopy (APXPS). This technique provides quantitative information on, e.g., functional groups at surfaces under relevant relative humidity conditions and allows for distinguishing between the oxygen atoms of the oxide, hydroxyl groups, and molecular water.^{4,5}

Over the past two decades, a growing library of APXPS water adsorption studies on metal oxides under relevant humidity conditions have been published, including investigations on single crystals,^{6–9} epitaxial films,^{10–16} and polycrystalline metal oxide.^{17–22} While the specifics of surface hydroxylation and water adsorption depend on the crystalline face and amount of surface defects, a few general trends emerge from these studies; for instance, hydroxyl groups form on polycrystalline surfaces at lower RH than on single-crystalline surfaces. An intriguing observation is that on most well-ordered, single-crystalline surfaces, a common onset threshold of 0.01% RH for terrace site hydroxylation is observed, accompanied by the adsorption onset of molecular water. This trend seems to indicate that surface hydroxylation is a prerequisite for molecular water adsorption.

Received: April 30, 2019

Revised: June 17, 2019

Published: June 20, 2019

MoO₃ presents an interesting test case for these general trends. Here, we present the results of coupled APXPS measurements of a MoO₃ film and density functional theory (DFT) calculations of the energetically preferred (010) surface. Figure 1 shows the MoO₃ bilayer structure, which is

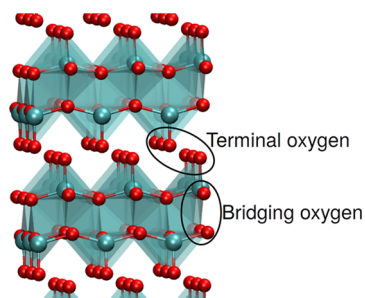


Figure 1. Crystal structure of MoO₃(010) contains bilayers of octahedrally coordinated Mo atoms and an oxygen-terminated surface. O atoms are shown in red and Mo in cyan.

characterized by coordinatively saturated Mo⁶⁺ ions, with no open adsorption sites at the metal atoms. There are two lone pairs of electrons on terminal oxygen atoms that could act as a hydrogen acceptor for water adsorption. Despite this possibility, we will show that there is neither significant surface hydroxylation nor molecular water adsorption at these terminal O atoms. Previous theoretical calculations already showed that the interaction of single water molecules with stoichiometric, oxygen-terminated MoO₃(010) is indeed weak, with adsorption energies on the order of a few hundred meV.²³ However, strong water adsorption has been shown in calculations on model clusters where water was found to occupy an oxygen vacancy site.²⁴ A different theoretical study showed that water adsorbs on a (100) surface, which has coordinately unsaturated Mo atoms.²⁵ The calculations performed in this work confirm that the unavailability of metal centers for adsorption leads to the hydrophobicity of the MoO₃(010) surface.

2. METHODS

2.1. APXPS Experiments. The experiments were performed using the APXPS-1 endstation²⁶ of beamline 11.0.2²⁷ at the Advanced Light Source, Berkeley, CA. The endstation is equipped with a preparation and an analysis chamber, both with base pressures typically at or below 2×10^{-9} Torr. A differentially pumped electron analyzer system (modified Phoibos 150, Specs Surface Nanoanalysis GmbH, Berlin) is attached to the analysis chamber; electrons and gas molecules enter the electron analyzer lens through a differentially pumped aperture with a diameter of $\sim 200 \mu\text{m}$.²⁸ The electrons are collected under the magic angle (55°) to the incident photons. Typical aperture sample distances are on the order of 1 mm to reduce elastic and inelastic scattering of electrons by the gas phase.

The MoO₃ sample was prepared by oxidizing a commercially available Mo foil (Alpha Aesar, 99.95%) with a diameter of ~ 1 cm, which was first cleaned via sequential sonication in ethanol and Millipore-grade water. Subsequently, the foil was transferred into the preparation chamber and further cleaned in vacuum via Ar⁺ sputtering (1×10^{-5} Torr Ar⁺, 5 mA, 1.5 keV, 15 min), followed by annealing to 900 °C for 15 min. A MoO₃ surface was then prepared by heating the clean foil to 435 °C in 35 Torr of O₂ for 10 min, followed by cooling to 100 °C in

the same oxygen pressure. Water vapor was provided by a liquid water source, which was degassed via at least three freeze–pump–thaw cycles and then admitted into the analysis chamber with a precision leak valve. Since water is known to crack on hot ion gauge filaments,^{4,17} care was taken that the filament of the ion gauge was cooled down in the experiments at pressures below 10^{-4} Torr. For the pressure of $<10^{-4}$ Torr, the water vapor pressure was calibrated beforehand without the presence of the sample, where the number of turns of the leak valve was correlated with the ion gauge reading; several of these calibrations were performed before and after each experiment to ensure reproducibility. The maximum water pressure was 1 Torr (6% RH), as the increased scattering of photoelectrons by the gas phase at higher pressures results in a decrease in the signal. The temperature of the sample was 20 °C during data collection unless mentioned otherwise; the relative humidity is a function of sample temperature and water vapor pressure. Photoelectron spectra were obtained at a kinetic energy of ~ 200 eV, which ensures the same sampling depth for each core level and the same collection efficiency (gas-phase attenuation, lens transmission). To that end, incident photon energies of 735 eV for O 1s and 435 eV for Mo 3d spectra were used. The binding energy axis in each spectrum is calibrated to the position of the Mo 3d_{5/2} peak at 232.5 eV;²⁹ to calibrate the O 1s spectra, Mo 3d_{5/2} spectra were also collected at 735 eV. The combined beamline and analyzer resolution was better than 350 meV. To prevent photon-induced changes to the sample,³⁰ using a new position on the sample for each spectrum was found to be sufficient, as we have reported previously.³

2.2. Calculations. Though the crystalline phase of the MoO₃ film was not characterized in the experiments, the most energetically favorable MoO₃(010) surface was chosen for modeling. DFT calculations within the periodic supercell approach as implemented in the Vienna ab initio simulation package were performed.³¹ The vdW-DF2³² functional was used throughout, as it has been shown, from a range of van der Waals inclusive functionals, to give the best interlayer distance for MoO₃.³³ The inner electrons were replaced by projector-augmented wave potentials,³⁴ whereas the valence states were expanded in plane waves with a cutoff energy of 700 eV. We used a Monkhorst–Pack *k*-point grid of $5 \times 1 \times 5$ for the bulk. The Hubbard parameter, *U*, was employed in the Dudarev approach³⁵ to treat the onsite coulomb interaction in the 4d Mo electrons. A *U*–*J* value between 3 and 7 was tested and found to have only a moderate effect on the band-gap value, which increases from 1.6 eV (*U*–*J* = 3 eV) to 2.1 eV (*U*–*J* = 7 eV); this small effect results from the d⁰ configuration of the Mo 4d orbitals. Following the work of Coquet et al.,³⁶ we calculated the spin density on a MoO₃(010) surface (modeled by a $3 \times 1 \times 3$ slab with 15 Å of vacuum between periodic images in the *y*-direction; the bottom O–Mo–O layers are kept fixed) with a terminal oxygen removed. A spin density of 1.98 is obtained for *U*–*J* = 5, which is close to the density of 1.96 obtained by Coquet et al. with a hybrid functional in a cluster model;³⁶ thus, we used *U*–*J* = 5. The lattice parameters for the bulk with these settings are *a* = 3.78 Å, *b* = 14.3 Å, and *c* = 3.90 Å, with a 1.9, 1.3, and –1.7% errors, respectively, from the experimental values.^{37,38} Adsorption calculations of monomers of water were performed, considering (2 × 2) slabs cut along the MoO₃(010) direction consisting of one single MoO₃ sheet and separated by 15 Å of vacuum. Tests with two sheets showed a relaxed surface structure, which was

identical to that obtained when using only one slab; so, the latter model was employed. In all cases, the bottom O–Mo–O layers were kept fixed to the bulk positions. A dipole correction along the direction perpendicular to the metal surface was applied, and geometry optimizations were performed with a residual force threshold of $0.005 \text{ eV } \text{\AA}^{-1}$. The adsorption energy, E_{ads} is calculated using a standard definition: $E_{\text{ads}} = (E_{\text{total}} - E_{\text{substrate}} - nE_{\text{H}_2\text{O}})/n$, where E_{total} is the energy of the adsorbed system, $E_{\text{substrate}}$ is the energy of the MoO_3 slab (which can be stoichiometric, contain an O vacancy, or contain a hydroxyl group), and $E_{\text{H}_2\text{O}}$ is the energy of a water molecule in the gas phase.

3. RESULTS

3.1. Ambient Pressure X-ray Photoelectron Spectroscopy. Figure 2a shows the Mo $3d_{5/2}$ spectrum of a freshly

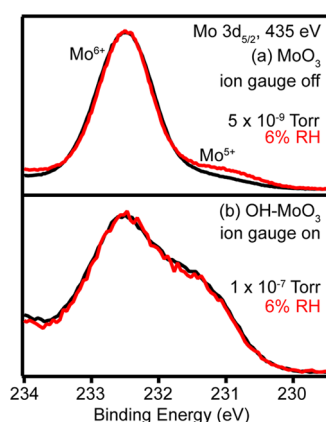


Figure 2. Mo $3d_{5/2}$ photoelectron spectra of (a) MoO_3 under UHV (black) show Mo^{6+} at 232.5 eV and a small amount of Mo^{5+} at ~231 eV, which increases at 6% RH (red). (b) The OH-MoO_3 surface (black) was prepared by the immediate hydroxylation of some of the oxygen defects (i.e., Mo^{5+}) that were generated by gentle sputtering. The Mo states of OH-MoO_3 do not change under 6% RH (red). See the text for an explanation of the ion gauge.

prepared MoO_3 surface (black trace). Besides the main Mo^{6+} peak (232.5 eV), a smaller peak at lower binding energy (~231 eV) indicates some Mo^{5+} ,²⁹ which is likely due to inhomogeneities in the metal foil substrate that introduce defects in the MoO_3 film. The corresponding O 1s peak of the oxide is shown in Figure 3a (black trace) and is located at the commonly reported literature value for its binding energy of 530.3 eV.²⁹ The slight asymmetry at the high binding energy of the peak suggests that there may be some hydroxyl groups on the surface.

After the measurement of the as-prepared samples, they were exposed to water vapor. The water vapor was dosed into the analysis chamber of the APXPS in increasing steps of 1 order of magnitude at a time, starting from 1×10^{-7} Torr (Figures S1 and S2). The red trace in Figure 3a shows the O 1s spectrum at the highest RH of 6% (1 Torr H_2O at 20 °C). There is no significant increase in surface hydroxylation or molecular water adsorption, both of which are expected to manifest themselves in peaks at the high-binding-energy shoulder of the oxide O 1s peak.⁶ The only observable change is the presence of the water vapor O 1s peak at an apparent binding energy of ~534 eV. The comparison of the O 1s spectra of MoO_3 under UHV conditions (black) and under 6%

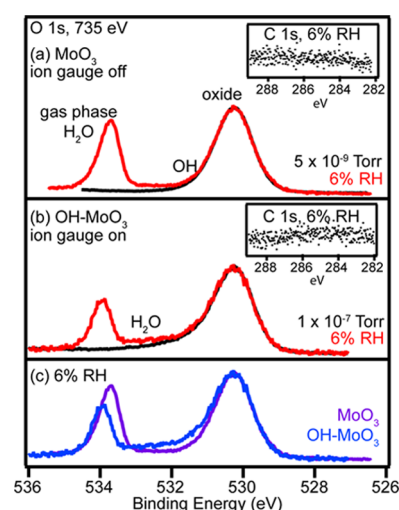


Figure 3. O 1s photoelectron spectrum of (a) MoO_3 under UHV (black) shows a small amount of asymmetry on the high-binding-energy side, which could indicate surface hydroxyl groups. At 6% RH (red), there is no increase in hydroxyl groups, no significant adsorption of molecular water, and no adventitious carbon adsorption. (b) Water exposure of a surface into which defects were introduced through sputtering (OH-MoO_3) shows increased amounts of adsorbed molecular water at low RH (black) and results in slightly more adsorption at 6% RH (red). (c) OH-MoO_3 surface (blue) has more adsorbed water than the pristine MoO_3 (purple) at 6% RH. See the text for an explanation of the ion gauge.

RH (red) in Figure 3a only shows a slight intensity increase in the raw data of around 532 eV, the binding energy of molecular water on an oxide surface.^{6,12,17} However, after subtraction of a Shirley-type background, this apparent peak is not observed anymore. Within the confines of this experiment and the data analysis, it is difficult to distinguish if the increased count rate at ~532 eV is due to an additional peak from adsorbed water or due to other effects brought upon by the presence of the gas phase, such as scattering of electrons by gas molecules.

The lack of significant water adsorption on the pristine MoO_3 surface was found to be reproducible. We also tested the influence of a hot ion gauge filament on the results; as was demonstrated in other systems, a hot filament often causes cracking of gaseous species, including molecular water, resulting in an increase of surface hydroxylation of some metal oxides.¹⁷ However, the O 1s spectra recorded during water dosing with the ion gauge on (Figures S6 and S7) are nearly identical, highlighting the hydrophobicity and inertness of MoO_3 . Since the ion gauge was not found to influence hydroxylation and water adsorption in this case, we show the O 1s spectrum for OH-MoO_3 at 6% RH with the ion gauge on in Figure 3b so that the MoO_3 and the OH-MoO_3 surfaces are compared under the same humidity conditions.

While the O 1s spectrum does not show changes upon an increase of the RH, the Mo $3d_{5/2}$ spectrum exhibits a small growth of the Mo^{5+} shoulder when the RH is raised to 6% (see Figure 2a). Higher amounts of Mo^{5+} are indicative of an increase in the number of oxygen vacancies. However, it is expected that oxygen vacancies at the surface are quickly filled by a reaction with water molecules from the vapor and the subsequent formation of hydroxyl groups.⁶ The increase in Mo^{5+} could be caused by beam-induced reduction of the oxide (despite attempts to prevent this from happening) and by

oxygen vacancies in the subsurface region of the sample that are slower to heal.³⁹

Interestingly, no carbon accumulates on the surface in the presence of water vapor, which is contrary to the general observation in many other experiments at elevated RH, where reduced pumping combined with the mobilization of carbonaceous species from the chamber walls leads to detectable C 1s signals in most cases.^{4,17} This carbon accumulation is not observed here for MoO₃, as the insets with the C 1s spectra in Figure 3 show. Even at 6% RH, the surface is devoid of detectable amounts of carbonaceous species.

Following the investigations of the pristine MoO₃ surface, we now turn our attention to the effect of deliberately introduced surface defects on the interaction with water vapor. As we have reported in another MoO₃ study,³ defects were introduced on the surface by gentle Ar⁺ sputtering, which are then hydroxylated by background water in the chamber; we label this surface OH–MoO₃. The results are shown in Figures 2b and 3b. The Mo 3d_{5/2} spectra in Figure 2b show the reduction of Mo⁶⁺ to Mo⁵⁺ due to sputtering when compared with the spectra of the pristine surface in Figure 2a. The spectra are very similar in vacuum (black) and at 6% RH, indicating that all surface reactions have already run their course under very low RH conditions. The O 1s spectra in Figure 3b show an increase in the hydroxyl groups under vacuum conditions (black trace) when compared to the pristine surface (Figure 3a). Additionally, there is noticeable molecular water on the surface already under vacuum conditions. Upon increasing the RH to 6%, only a small additional amount of water adsorbs (red trace in Figure 3b). Figure 3c overlays the pristine MoO₃ and OH–MoO₃ O 1s spectra at 6% RH, further highlighting the slight increase of water adsorption on the OH–MoO₃ surface. Overall, the experimental results show that the introduction of defects (oxygen vacancies) through sputtering increases the number of hydroxyl groups at the surface, which, in turn, results in an increase in the adsorption of molecular water. However, in stark contrast to other metal oxide surfaces,^{6–9,11,13,14,16–19,22} the amount of hydroxyl groups and water at the surface at elevated RH is still small, pointing to a weak interaction of water with MoO₃. To understand this phenomenon better, we next employ DFT to model the reaction.

3.2. Density Functional Theory Calculations. To gain more insight into the hydrophobic properties of MoO₃ and the role of its electronic structure in water adsorption, DFT calculations were performed. The surface crystallinity of the oxide film in the experiments was not characterized; so, the most stable MoO₃(010) surface was chosen for modeling. Calculations on this surface have proven sufficient to help interpret other APXPS data on similar MoO₃ samples.³ On the fully O-terminated surface, water molecules weakly adsorb via the interaction between the water H atoms and the surface terminal O atoms (see Figure 4a). The adsorption energy is calculated as –0.31 eV. The weak adsorption energy correlates well with the minimal overlapping of the Mo d and O p states, as seen in the partial density of states (DOS) graph in Figure 4a. Dissociation is never favorable on the stoichiometric surface.

The possibility for strong water adsorption is found on a surface with a terminal oxygen vacancy. The change in stoichiometry introduces an additional surface state (see Figure S8). Surface states due to defects have been shown to alter the reactivity in other oxide surfaces.^{40,41} In this case, the water O

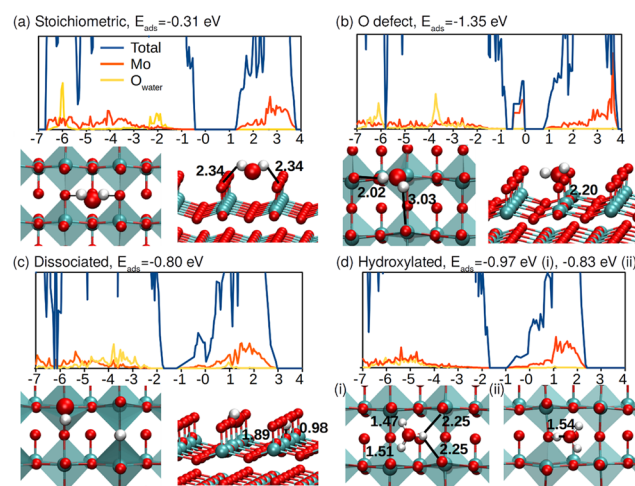


Figure 4. Structure, adsorption energies (E_{ads}), and density of state plots for four stable structures found on MoO₃(010). Water weakly adsorbs on (a) a stoichiometric O-terminated surface and more strongly adsorbs on (b) a surface with an O vacancy. (c) Dissociative water adsorption is favorable on a surface with an O vacancy. (d) Water adsorption on a surface with a hydroxyl group on terminal oxygen is also possible. In the graphs, the lines are DOS in electron volts: blue is the total DOS, orange is Mo d states, and yellow is O p states. O atoms are shown in red, H atoms in white, and Mo atoms in cyan. In the top-down view, the octahedral cages around the top layer Mo atoms are also shown. Adsorbed species (H₂O, H) are shown in a larger size for clarity. The numbers on the structures indicate interatomic distances in Å.

atom takes the place of the missing lattice oxygen, while the two H atoms interact with neighboring terminal oxygens (see Figure 4b). The calculated adsorption energy for this geometry is –1.35 eV. A stronger overlap between the Mo d and O p states is seen, with the O_{water} peak in the DOS shifting by –2 eV from its value for the stoichiometric surface (Figure 4a) to nearly –4 eV when a terminal oxygen vacancy is introduced (Figure 4b). The introduction of oxygen vacancies encourages water dissociation, with adsorption energies ranging from –0.65 to –0.80 eV. These structures include the formation of two surface hydroxyl groups and, in the most stable structure, a H atom binding to the bridging O between two Mo atoms (Figure 4c). These dissociated structures are still energetically less favorable than the one where an intact water molecule fills an oxygen vacancy (Figure 4b) but are sufficiently stable to be likely observed. In addition, surface hydroxylation provides a certain degree of stabilization of adsorbed water molecules on MoO₃(010); a range of stable configurations with molecular water bound to a surface hydroxyl group were found, with adsorption energies ranging from –0.7 to –0.97 eV. The most stable configurations are shown in Figure 4d (and more extensively in Figure S10). The most stable structure (Figure 4d,i) sees the formation of a hydronium molecule, a species that has been previously observed in water adsorption of hydroxylated oxide and metal surfaces.^{42,43} Other configurations show, instead, the adsorption of the water molecule to a hydroxyl formed on bridging oxygen. Despite the strong adsorption of water on the hydroxylated surface, dissociation is hindered, and no stable structures are found when coadsorbing an OH group and a H atom. Similar to dissociation on the stoichiometric surface, there is no stable adsorption site for the OH group on the surface O atoms, while the adsorption of an

OH onto a hydroxyl group leads to a recombination of the two into a H_2O molecule.

4. DISCUSSION

The low propensity for water adsorption and dissociation on $\text{MoO}_3(010)$ stands in stark contrast to a long list of metal oxide surfaces, where widespread hydroxylation and water adsorption occurs at around 0.01% RH. As the APXPS data show, despite relative humidity conditions that exceed this threshold by nearly 3 orders of magnitude (6% RH), no significant amount of water adsorption or hydroxylation was seen in the APXPS data of the pristine MoO_3 sample. When the surface has more hydroxyl groups produced through sputtering and creation of oxygen vacancies, a higher coverage by molecular water is observed under vacuum conditions (10^{-7} Torr, where the dominant gas-phase component is water); however, no substantial additional water adsorption occurs upon increasing the relative humidity to 6%. DFT calculations of water adsorption on the $\text{MoO}_3(010)$ surface agree with these experimental observations. As shown in Figure 1, crystalline MoO_3 is a bilayer structure, with van der Waals interactions between adjacent (010) layers. The (010) surface contains solely oxygen atoms that are double-bonded to the Mo atoms in the second atomic layer, which likely stabilizes the surface oxygens so that protonation and consequently hydroxyl group formation are energetically not favored. However, the formation of hydrogen bonds with water molecules through the lone-pair electrons of the surface oxygen atoms appears to be somewhat favorable, as the DFT calculations (Figure 4a) show. The most stable, but still relatively weak, interaction of water with the stoichiometric surface is through hydrogen bonding with the terminal oxygen atoms. However, the calculations do not predict water dissociation on the stoichiometric surface.

A strong adsorption site for molecular water on metal oxides is an exposed unsaturated metal atom, where the water–metal interaction is mediated via the O lone pairs.⁴⁴ A general rule has not yet been established for the occurrence of water dissociation on an oxide. However, the water interaction with metal cations appears to be of central importance, and stronger water–metal interactions are linked to more acidic O–H protons that are more prone to dissociation.⁴⁴ This observation is similar to what has been established for the interaction of water with metals, where there is a delicate balance between water adsorption strength and degree of dissociation.⁴⁵ The position of the O 2p levels with respect to the oxide band gap has also been shown to be indicative of the propensity of a surface for water dissociation.⁴⁶ The O 1s spectra of the sputtered surface show that more hydroxyl groups are present than on the stoichiometric surface, most likely due to the dissociation of background water at open metal sites already under vacuum conditions. DFT results are consistent with both the experimental observations and the literature, showing that water adsorption favors open metal sites at which dissociation readily proceeds.

The observations from our APXPS and DFT study are consistent with the findings of Sian and Reddy, who studied the hydroxylation and water adsorption of MoO_3 films with different microstructures and stoichiometries using infrared spectroscopy.⁴⁷ They found that the most stoichiometric and polycrystalline film neither adsorbed water nor hydroxylated even after exposure to 70% RH for 40 days. The amorphous, less stoichiometric films formed hydroxyl groups and adsorbed

water after a day of exposure to 70% RH, likely due to the higher concentration of defects in the film. It is also remarkable that in our APXPS studies we did not see any signs of hydrocarbon adsorption throughout our experiments. This observation is contrary to the overwhelming number of water adsorption studies that have been performed previously using APXPS that showed detectable amounts of carbonaceous species, especially at elevated humidity. While the surface chemistry of MoO_3 with respect to hydrocarbon species was not the focus of this study, it is noteworthy that MoO_3 shows significant inertness not only toward water but also toward other small carbonaceous molecules (e.g., CO, CO_2) that are typically components of the residual gas inside a vacuum chamber.

5. CONCLUSIONS

APXPS results show that a MoO_3 film does not extensively adsorb water or form hydroxyl groups under RH conditions up to 6% due to the stability of the terminal oxygen atoms at the surface. Increasing the surface hydroxyl group coverage by the introduction of oxygen vacancies, i.e., unsaturated metal sites, via sample preparation methods only slightly increases water adsorption. DFT studies on the $\text{MoO}_3(010)$ surface agree with experimental results, showing that only a weak van der Waals interaction occurs between the water H atoms and surface terminal oxygen atoms. The strength of this interaction increases when oxygen vacancies or hydroxyl groups are present on the surface. Water dissociation is favorable only when water adsorbs to an unsaturated Mo site through the oxygen atom in water. These results have implications in gas-filtering technology, where the defect concentration of MoO_x particles in porous carbon will play a role in the amount of water that is adsorbed. Furthermore, the extent of hydroxylation could factor in chemistry involving both adsorption targets and atmospheric gases.

■ ASSOCIATED CONTENT

Supporting Information

The Supporting Information is available free of charge on the ACS Publications website at DOI: 10.1021/acs.jpcc.9b03822.

Mo $3d_{5/2}$ spectra (Figure S1); O 1s spectra (Figure S2); C 1s spectra (Figure S3); Mo $3d_{5/2}$ spectra of MoO_3 (Figure S4); Mo $3d_{5/2}$ spectra of OH– MoO_3 (Figure S5); O 1s spectra of MoO_3 (Figure S6); O 1s spectra of OH– MoO_3 (Figure S7); DOS and pDOS for clean surfaces (Figure S8); total density of states for surfaces with adsorbed H_2O (Figure S9); structure and adsorption energies of the most stable H_2O adsorption structures (Figure S10); and coordinates for calculated structures (PDF)

■ AUTHOR INFORMATION

Corresponding Author

*E-mail: hbluhm@lbl.gov, bluhm@fhi-berlin.mpg.de. Phone: +49-30-8413 4633.

ORCID

Ashley R. Head: 0000-0001-8733-0165

Chiara Gattinoni: 0000-0002-3376-6374

Lena Trotochaud: 0000-0002-8816-3781

Yi Yu: 0000-0003-1667-5187

Osman Karşlıoğlu: 0000-0003-4018-4572

Sven Pletincx: 0000-0003-4070-6019

Bryan Eichhorn: 0000-0001-9161-1920

Present Addresses

[○]Center for WaSH-AID, Duke University, Durham, North Carolina 27701, United States (L.T.).

[◆]Condensed Matter Physics and Photon Science Division, ShanghaiTech University, Shanghai 201210, China (Y.Y.).

[†]Department of Interface Science, Fritz Haber Institute of the Max Planck Society, Faradayweg 4-6, D-14195 Berlin, Germany (O.K.).

Notes

The authors declare no competing financial interest.

ACKNOWLEDGMENTS

Support by the Defense Threat Reduction Agency under grant number HDTRA11510005 is gratefully acknowledged. The ALS and the MES beamline 11.0.2 are supported by the Director, Office of Science, Office of Basic Energy Sciences, Division of Chemical Sciences, Geosciences, and Biosciences and Materials Sciences Division of the U.S. Department of Energy at the Lawrence Berkeley National Laboratory under Contract DE-AC02-05CH11231. C.G. is supported by the European Union's Horizon 2020 research and innovation program under the Marie Skłodowska-Curie grant agreement No. 744027. This work was supported by a grant from the Swiss National Supercomputing Centre (CSCS) under project ID s798. A.R.H. acknowledges support from the Center for Functional Nanomaterials, which is a U.S. DOE Office of Science Facility, at Brookhaven National Laboratory under Contract No. DE-SC0012704. Roman Tsyshevskiy and Maija M. Kuklja are gratefully acknowledged for fruitful discussions.

REFERENCES

- (1) Björneholm, O.; Hansen, M. H.; Hodgson, A.; Liu, L.-M.; Limmer, D. T.; Michaelides, A.; Pedevilla, P.; Rossmel, J.; Shen, H.; Tocci, G.; et al. Water at Interfaces. *Chem. Rev.* **2016**, *116*, 7698–7726.
- (2) Morrison, R. W. *NBC Filter Performance*, ECBC-TR-135; U.S. Army Soldier and Biological Chemical Command: Aberdeen Proving Grounds, MD, 2001.
- (3) Head, A. R.; Tsyshevsky, R.; Trotochaud, L.; Yu, Y.; Kyhl, L.; Karşioğlu, O.; Kuklja, M. M.; Bluhm, H. Adsorption of Dimethyl Methylphosphonate on MoO₃: The Role of Oxygen Vacancies. *J. Phys. Chem. C* **2016**, *120*, 29077–29088.
- (4) Trotochaud, L.; Head, A. R.; Karşioğlu, O.; Kyhl, L.; Bluhm, H. Ambient Pressure Photoelectron Spectroscopy: Practical Considerations and Experimental Frontiers. *J. Phys.: Condens. Matter* **2017**, *29*, No. 053002.
- (5) Starr, D. E.; Liu, Z.; Hävecker, M.; Knop-Gericke, A.; Bluhm, H. Investigation of Solid/Vapor Interfaces Using Ambient Pressure X-Ray Photoelectron Spectroscopy. *Chem. Soc. Rev.* **2013**, *42*, 5833.
- (6) Ketteler, G.; Yamamoto, S.; Bluhm, H.; Andersson, K.; Starr, D. E.; Ogletree, D. F.; Ogasawara, H.; Nilsson, A.; Salmeron, M. The Nature of Water Nucleation Sites on TiO₂ (110) Surfaces Revealed by Ambient Pressure X-Ray Photoelectron Spectroscopy. *J. Phys. Chem. C* **2007**, *111*, 8278–8282.
- (7) Stoerzinger, K. A.; Hong, W. T.; Crumlin, E. J.; Bluhm, H.; Biegalski, M. D.; Shao-Horn, Y. Water Reactivity on the LaCoO₃(001) Surface: An Ambient Pressure X-Ray Photoelectron Spectroscopy Study. *J. Phys. Chem. C* **2014**, *118*, 19733–19741.
- (8) Yamamoto, S.; Kendelewicz, T.; Newberg, J. T.; Ketteler, G.; Starr, D. E.; Mysak, E. R.; Andersson, K. J.; Ogasawara, H.; Bluhm, H.; Salmeron, M.; et al. Water Adsorption on α -Fe₂O₃ (0001) at near Ambient Conditions. *J. Phys. Chem. C* **2010**, *114*, 2256–2266.
- (9) Schaefer, A.; Lanzilotto, V.; Cappel, U.; Uvdal, P.; Borg, A.; Sandell, A. First Layer Water Phases on Anatase TiO₂(101). *Surf. Sci.* **2018**, *674*, 25–31.
- (10) Kraus, T. J.; Nepomnyashchii, A. B.; Parkinson, B. A. Atomic Layer Deposition of Epitaxial Layers of Anatase on Strontium Titanate Single Crystals: Morphological and Photoelectrochemical Characterization. *J. Vac. Sci. Technol., A* **2015**, *33*, No. 01A135.
- (11) Newberg, J. T.; Starr, D. E.; Yamamoto, S.; Kaya, S.; Kendelewicz, T.; Mysak, E. R.; Porsgaard, S.; Salmeron, M. B.; Brown, G. E.; Nilsson, A.; et al. Formation of Hydroxyl and Water Layers on MgO Films Studied with Ambient Pressure XPS. *Surf. Sci.* **2011**, *605*, 89–94.
- (12) Newberg, J. T.; Starr, D. E.; Yamamoto, S.; Kaya, S.; Kendelewicz, T.; Mysak, E. R.; Porsgaard, S.; Salmeron, M. B.; Brown, G. E.; Nilsson, A.; et al. Autocatalytic Surface Hydroxylation of MgO(100) Terrace Sites Observed under Ambient Conditions. *J. Phys. Chem. C* **2011**, *115*, 12864–12872.
- (13) Shavorskiy, A.; Müller, K.; Newberg, J. T.; Starr, D. E.; Bluhm, H. Hydroxylation of Ultrathin Al₂O₃/NiAl(110) Films at Environmental Humidity. *J. Phys. Chem. C* **2014**, *118*, 29340–29349.
- (14) Stoerzinger, K. A.; Comes, R.; Spurgeon, S. R.; Thevuthasan, S.; Ihm, K.; Crumlin, E. J.; Chambers, S. A. Influence of LaFeO₃ Surface Termination on Water Reactivity. *J. Phys. Chem. Lett.* **2017**, *8*, 1038–1043.
- (15) Deng, X.; Lee, J.; Wang, C.; Matranga, C.; Aksoy, F.; Liu, Z. Reactivity Differences of Nanocrystals and Continuous Films of α -Fe₂O₃ on Au(111) Studied with In Situ X-Ray Photoelectron Spectroscopy. *J. Phys. Chem. C* **2010**, *114*, 22619–22623.
- (16) Kendelewicz, T.; Kaya, S.; Newberg, J. T.; Bluhm, H.; Mulakaluri, N.; Moritz, W.; Scheffler, M.; Nilsson, A.; Pentcheva, R.; Brown, G. E. X-Ray Photoemission and Density Functional Theory Study of the Interaction of Water Vapor with the Fe₃O₄(001) Surface at Near-Ambient Conditions. *J. Phys. Chem. C* **2013**, *117*, 2719–2733.
- (17) Trotochaud, L.; Head, A. R.; Pletincx, S.; Karşioğlu, O.; Yu, Y.; Waldner, A.; Kyhl, L.; Hauffman, T.; Terryn, H.; Eichhorn, B.; et al. Water Adsorption and Dissociation on Polycrystalline Copper Oxides: Effects of Environmental Contamination and Experimental Protocol. *J. Phys. Chem. B* **2018**, *122*, 1000–1008.
- (18) Deng, X.; Herranz, T.; Weis, C.; Bluhm, H.; Salmeron, M. Adsorption of Water on Cu₂O and Al₂O₃ Thin Films. *J. Phys. Chem. C* **2008**, *112*, 9668–9672.
- (19) Mura, A.; Hidesima, I.; Liu, Z.; Hosoi, T.; Watanabe, H.; Arima, K. Water Growth on GeO₂/Ge(100) Stack and Its Effect on the Electronic Properties of GeO₂. *J. Phys. Chem. C* **2013**, *117*, 165–171.
- (20) Jribi, R.; Barthel, E.; Bluhm, H.; Grunze, M.; Koelsch, P.; Verreault, D.; Søndergård, E. Ultraviolet Irradiation Suppresses Adhesion on TiO₂. *J. Phys. Chem. C* **2009**, *113*, 8273–8277.
- (21) Stoerzinger, K. A.; Hong, W. T.; Azimi, G.; Giordano, L.; Lee, Y.-L.; Crumlin, E. J.; Biegalski, M. D.; Bluhm, H.; Varanasi, K. K.; Shao-Horn, Y. Reactivity of Perovskites with Water: Role of Hydroxylation in Wetting and Implications for Oxygen Electrocatalysis. *J. Phys. Chem. C* **2015**, *119*, 18504–18512.
- (22) Rameshan, C.; Ng, M. L.; Shavorskiy, A.; Newberg, J. T.; Bluhm, H. Water Adsorption on Polycrystalline Vanadium from Ultra-High Vacuum to Ambient Relative Humidity. *Surf. Sci.* **2015**, *641*, 141–147.
- (23) Yin, X.; Han, H.; Miyamoto, A. Structure and Adsorption Properties of MoO₃: Insights from Periodic Density Functional Calculations. *J. Mol. Model.* **2001**, *7*, 207–215.
- (24) Song, X.; Liu, G.; Yu, J.; Rodrigues, A. E. Density Functional Theoretical Study of Water Molecular Adsorption on Surface of MoO₃ with the Cluster Model. *J. Mol. Struct.: THEOCHEM* **2004**, *684*, 81–85.
- (25) Papakondylis, A.; Sautet, P. *Ab Initio* Study of the Structure of the α -MoO₃ Solid and Study of the Adsorption of H₂O and CO Molecules on Its (100) Surface. *J. Phys. Chem. A* **1996**, *100*, 10681–10688.

- (26) Frank Ogletree, D.; Bluhm, H.; Hebenstreit, E. D.; Salmeron, M. Photoelectron Spectroscopy under Ambient Pressure and Temperature Conditions. *Nucl. Instrum. Methods Phys. Res., Sect. A* **2009**, *601*, 151–160.
- (27) Bluhm, H.; Andersson, K.; Araki, T.; Benzerara, K.; Brown, G. E.; Dynes, J. J.; Ghosal, S.; Gilles, M. K.; Hansen, H.-C.; Hemminger, J. C.; et al. Soft X-Ray Microscopy and Spectroscopy at the Molecular Environmental Science Beamline at the Advanced Light Source. *J. Electron Spectrosc. Relat. Phenom.* **2006**, *150*, 86–104.
- (28) Ogletree, D. F.; Bluhm, H.; Lebedev, G.; Fadley, C. S.; Hussain, Z.; Salmeron, M. A Differentially Pumped Electrostatic Lens System for Photoemission Studies in the Millibar Range. *Rev. Sci. Instrum.* **2002**, *73*, 3872–3877.
- (29) Scanlon, D. O.; Watson, G. W.; Payne, D. J.; Atkinson, G. R.; Egddell, R. G.; Law, D. S. L. Theoretical and Experimental Study of the Electronic Structures of MoO₃ and MoO₂. *J. Phys. Chem. C* **2010**, *114*, 4636–4645.
- (30) Liao, X.; Jeong, A. R.; Wilks, R. G.; Wiesner, S.; Rusu, M.; Bär, M. X-Ray Irradiation Induced Effects on the Chemical and Electronic Properties of MoO₃ Thin Films. *J. Electron Spectrosc. Relat. Phenom.* **2016**, *212*, 50–55.
- (31) Kresse, G.; Hafner, J. *Ab Initio* Molecular Dynamics for Liquid Metals. *Phys. Rev. B* **1993**, *47*, 558–561.
- (32) Klimeš, J.; Bowler, D. R.; Michaelides, A. Chemical Accuracy for the van Der Waals Density Functional. *J. Phys.: Condens. Matter* **2010**, *22*, No. 022201.
- (33) Inzani, K.; Grande, T.; Vullum-Bruer, F.; Selbach, S. M. A van Der Waals Density Functional Study of MoO₃ and Its Oxygen Vacancies. *J. Phys. Chem. C* **2016**, *120*, 8959–8968.
- (34) Kresse, G.; Joubert, D. From Ultrasoft Pseudopotentials to the Projector Augmented-Wave Method. *Phys. Rev. B* **1999**, *59*, 1758–1775.
- (35) Dudarev, S. L.; Botton, G. A.; Savrasov, S. Y.; Humphreys, C. J.; Sutton, A. P. Electron-Energy-Loss Spectra and the Structural Stability of Nickel Oxide: An LSDA + U Study. *Phys. Rev. B* **1998**, *57*, 1505–1509.
- (36) Coquet, R.; Willock, D. J. The (010) Surface of α -MoO₃, a DFT + U Study. *Phys. Chem. Chem. Phys.* **2005**, *7*, 3819.
- (37) Negishi, H.; Negishi, S.; Kuroiwa, Y.; Sato, N.; Aoyagi, S. Anisotropic Thermal Expansion of Layered MoO₃ Crystals. *Phys. Rev. B* **2004**, *69*, No. 064111.
- (38) Sitepu, H. Texture and Structural Refinement Using Neutron Diffraction Data from Molybdate (MoO₃) and Calcite (CaCO₃) Powders and a Ni-Rich Ni_{50.70}Ti_{49.30} Alloy. *Powder Diffraction* **2009**, *24*, 315–326.
- (39) Scheiber, P.; Fidler, M.; Dulub, O.; Schmid, M.; Diebold, U.; Hou, W.; Aschauer, U.; Selloni, A. (Sub)Surface Mobility of Oxygen Vacancies at the TiO₂ Anatase (101) Surface. *Phys. Rev. Lett.* **2012**, *109*, No. 136103.
- (40) Kakekhani, A.; Ismail-Beigi, S. Ferroelectric Oxide Surface Chemistry: Water Splitting via Pyroelectricity. *J. Mater. Chem. A* **2016**, *4*, 5235–5246.
- (41) Hinuma, Y.; Toyao, T.; Kamachi, T.; Maeno, Z.; Takakusagi, S.; Furukawa, S.; Takigawa, I.; Shimizu, K. Density Functional Theory Calculations of Oxygen Vacancy Formation and Subsequent Molecular Adsorption on Oxide Surfaces. *J. Phys. Chem. C* **2018**, *122*, 29435–29444.
- (42) Grillo, M. E.; Finnis, M. W.; Ranke, W. Surface Structure and Water Adsorption on Fe₃O₄(111): Spin-Density Functional Theory and on-Site Coulomb Interactions. *Phys. Rev. B* **2008**, *77*, No. 075407.
- (43) Kizhakevariam, N.; Stuve, E. M. Coadsorption of Water and Hydrogen on Pt(100): Formation of Adsorbed Hydronium Ions. *Surf. Sci.* **1992**, *275*, 223–236.
- (44) Mu, R.; Zhao, Z.; Dohnálek, Z.; Gong, J. Structural Motifs of Water on Metal Oxide Surfaces. *Chem. Soc. Rev.* **2017**, *46*, 1785–1806.
- (45) Trasatti, S. Work Function, Electronegativity, and Electrochemical Behaviour of Metals. *J. Electroanal. Chem. Interfacial Electrochem.* **1972**, *39*, 163–184.
- (46) Xu, H.; Zhang, R. Q.; Ng, A. M. C.; Djurišić, A. B.; Chan, H. T.; Chan, W. K.; Tong, S. Y. Splitting Water on Metal Oxide Surfaces. *J. Phys. Chem. C* **2011**, *115*, 19710–19715.
- (47) Sian, T. S.; Reddy, G. B. Effect of Stoichiometry and Microstructure on Hydrolysis in MoO₃ Films. *Chem. Phys. Lett.* **2006**, *418*, 170–173.